Nonequilibrium superconductivity in spin-polarized superconducting tunneling junctions

Claudio Grimaldi*
Max-Planck-Institut für Physik Komplexer Systeme, Aussenstelle Stuttgart, Heisenbergstrasse 1, D-70569 Stuttgart, Germany

Peter Fulde
Max-Planck-Institut für Physik Komplexer Systeme, Bayreuther Strasse 40, D-01187 Dresden, Germany
(Received 24 January 1997)

The presence of an applied magnetic field can lead to important effects as regards the nonequilibrium properties of a superconductor when spin-flip scattering processes are taken into account. Here we consider spin-flip transitions due to spin-orbit scattering of the quasiparticles by impurities, and introduce the kinetic equations governing the quasiparticle and phonon excitations. We solve the kinetic equations for the case of a superconducting film in a magnetic field driven out of equilibrium by quasiparticle injection. We consider also two identical phonon-coupled superconducting tunneling junctions and calculate the current-voltage characteristics as a function of the applied magnetic field and the spin-orbit scattering rate. Our results provide a natural and simple interpretation of a recently reported experiment. [S0163-1829(97)00829-1]

I. INTRODUCTION

The study of the phenomenon of nonequilibrium superconductivity has led to interesting applications, especially in tunneling devices. A direct measurement of the quasiparticle recombination time, for example, has been obtained by means of superconducting tunneling junctions (STJ's) driven out of equilibrium by quasiparticle or phonon injection.[1–3] STJ's have also been used for quasimonochromatic phonon generation and detection,[4–8] and the corresponding physical processes have been studied extensively.[9–11] Recently, the time evolution towards a nonequilibrium state has also been investigated,[12] and a normal state junction has been successfully utilized as a phonon generator.[13]

The effects of magnetic fields on the properties of a nonequilibrium superconductor have also been investigated. Tunneling experiments on thin Al films have given evidence for the Zeeman splitting of the quasiparticle density of states (DOS),[14] and deviations from the BCS theory were successfully explained by electronic spin-flip processes induced by spin-orbit scattering with impurities.[15–18] By studying nonequilibrium phonons, it was shown that the quasimonochromatic emission of phonons can be tuned by varying the strength of the applied magnetic field.[6]

In a recently reported experiment,[19,20] an effect of the external magnetic field on the phonon generation and detection in ultrathin Al STJ's was observed. Namely, the detector-current–generator-voltage (I_D-V_G) characteristics of the phonon-coupled junctions (with equal energy gaps 2Δ) showed a dependence on the magnetic field H implying spin-flip transitions of the quasiparticles. In fact, in addition to the structures at $eV_G=2\Delta$ and $eV_G=4\Delta$ due to the onset of recombination and relaxation phonons,[8] an increase of the differential signal dI_D/dV_G was recorded also at $eV_G=2\Delta+2\mu_B H$ and $eV_G=4\Delta\pm2\mu_B H$, where μ_B is the Bohr magneton. The electron-phonon interaction responsible for the recombination and relaxation processes is spin conserving, and therefore the field-dependent signals must be ascribed to spin-flip transitions. A possible origin of such processes is found in the elastic spin-orbit scattering of the quasiparticles by impurities or surface effects.[21] In fact, the current-voltage characteristics of the tunneling junctions reported in Ref. 19 showed a clear signature of a small but finite value of the spin-orbit scattering rate. However, the observed small amount of spin-mixed states in the quasiparticle DOS due to spin-flip virtual processes, cannot provide an explanation for the field-dependent signals. Instead, the experimental data require a spin-flip collision integral of magnitude comparable to the one associated with the electron-phonon interaction. An interpretation of the experimental results based on this mechanism has already been reported.[21] Here, we clarify in greater details the physical processes involved in a nonequilibrium superconductor when the spin-orbit scattering is taken into account. Our analysis is based on a semiphenomenological approach in which the quasiparticle and phonon transitions are governed by the kinetic equations, the input parameters of which are extracted from the experimental data.

This article is organized as follows. In Sec. II we outline the properties of thin superconducting films in a magnetic field and in Sec. III we introduce and describe the kinetic equations for quasiparticles and phonons. In Sec. IV we solve the kinetic equations for a single tunneling junction in a magnetic field and study the nonequilibrium distributions of quasiparticles and phonons. In the same section we consider a system of two phonon-coupled identical STJ's in a magnetic field and discuss the effect of the spin-orbit scattering processes on the calculated differential detector-current I_D. The latter analysis is also an interpretation of the experimental data reported in Refs. 19,20.

II. SUPERCONDUCTING THIN FILMS IN A MAGNETIC FIELD

The physics of a superconductor under the influence of an external magnetic field H has been extensively studied in the past.[22] The magnetic field couples to the spin degrees of freedom via the electron magnetic moment and also influ-

ences the orbital motion of the quasiparticles. Both interactions break the time-reversal symmetry and lead to pair-breaking effects therefore suppressing superconductivity. In the following we focus on superconducting thin films in a magnetic field applied parallel to their surfaces. For film thicknesses of the size of 100 Å or less, the effect of the magnetic field on the electron spin becomes dominant. In an idealized situation in which the effect of the magnetic field on the electron orbital motion can be completely neglected, the quasiparticle excitation energy is given by $E_\sigma(\mathbf{p})=(\xi_p^2+\Delta^2)^{1/2}+\sigma\mu_B H$, where ξ_p is the normal electron energy measured from the chemical potential and $\sigma=\pm 1$. The corresponding density of states (DOS) per spin is of the BCS type, but shifted by the Zeeman energy $\sigma\mu_B H$:

$$N_\sigma(E)=\frac{N(0)}{2}\mathrm{sgn}(E)\mathrm{Re}\left\{\frac{E-\sigma\mu_B H}{[(E-\sigma\mu_B H)^2-\Delta^2]^{1/2}}\right\}, \quad (1)$$

where $N(0)$ is the density of states in the normal state at the Fermi energy summed over both spin directions.

The effect of the magnetic field on the orbital motion of the electrons leads to a modification of Eq. (1). Under the assumption that the following inequalities hold λ, $(\ell\xi_0)^{1/2}\gg d\gg\ell$, where λ and ξ_0 are the London penetration depth and the coherence length, respectively, and ℓ is the mean free path, the quasiparticle DOS becomes of the Abrikosov-Gorkov type,[16] which is given in units of $N(0)/2$ by

$$\rho_{\uparrow\downarrow}(E)=\mathrm{sgn}(E)\mathrm{Re}\left[\frac{u_\pm}{(u_\pm^2-1)^{1/2}}\right]. \quad (2)$$

$u_\pm$ is implicitly defined by the following algebraical equation:

$$\frac{E\mp\mu_B H}{\Delta}=u_\pm\left[1-\frac{\zeta}{(1-u_\pm^2)^{1/2}}\right], \quad (3)$$

where

$$\zeta=\frac{\tau_{\mathrm{tr}}(ev_F dH)^2}{18\Delta} \quad (4)$$

is the depairing parameter. Here, v_F is the Fermi velocity and τ_{tr} is the transport scattering time. For small values of ζ, the square root singularities in the DOS at $E\pm\mu_B H=\Delta$ are reduced to sharp peaks and the excitation threshold is shifted to lower energies. However, the spin is still a good quantum number and the Zeeman splitting is preserved. Note that when the film thickness goes to zero ($d\to 0$) the magnetic field has no effect on the electron orbital motion and the DOS becomes of BCS type as in Eq. (1). The order parameter Δ appearing in Eq. (3) is weakened by the presence of the depairing parameter ζ. At zero temperature and for $\zeta\ll 1$ it is found that[22]

$$\ln(\Delta/\Delta_0)=-\frac{\pi}{4}\zeta, \quad (5)$$

where Δ_0 is the order parameter in the absence of depairing effects ($\zeta=0$). For sufficiently small values of ζ, the order parameter can be approximated by its zero field value Δ_0 and we will limit our analysis to this case.

Spin-flip scattering processes can lead to important modifications of the excitation spectrum of a superconducting film. Such processes can be induced by magnetic impurities present in the film or spin-orbit scattering centers. Here, we consider only the latter mechanism, which originates from spin-orbit coupling to impurities or from strong electric fields arising near the boundaries of the film.[24] Regardless of the specific nature of the spin-orbit scattering, the usual procedure is to introduce an effective concentration n_i of scattering centers with a scattering potential of the form[16,17]

$$V(\mathbf{p},\mathbf{p}')=\frac{iv_{\mathrm{so}}}{p_F^2}(\mathbf{p}\times\mathbf{p}')\cdot\boldsymbol{\sigma}. \quad (6)$$

Here $\mathbf{p}$, $\mathbf{p}'$ are electronic momenta and $\boldsymbol{\sigma}$ is the spin vector operator. In the presence of the scattering potential (6), the electron spin is no longer a good quantum number and the electron will change its spin state during a characteristic time τ_{so} given by

$$\tau_{\mathrm{so}}^{-1}=\frac{1}{3}\frac{n_i}{\hbar}\frac{N(0)}{2}\int d\Omega|v_{\mathrm{so}}|^2\sin^2\theta. \quad (7)$$

The inclusion of the spin-orbit scattering time τ_{so} modifies the equations for the $u_\pm$ functions appearing in the DOS (2) in the following way:[16,17,22,23]

$$\frac{E\mp\mu_B H}{\Delta}=u_\pm\left[1-\frac{\zeta}{(1-u_\pm^2)^{1/2}}\right]+b_{so}\frac{u_\pm-u_\mp}{(1-u_\mp^2)^{1/2}}, \quad (8)$$

where $b_{\mathrm{so}}=\hbar/(\tau_{\mathrm{so}}\Delta)$ is the spin-orbit scattering parameter and ζ is again the depairing parameter given by Eq. (4).

The quasiparticle DOS for the two spin directions is reported in Fig. 1 for an applied magnetic field of 2 T and several values of the spin-orbit scattering parameter. When $b_{\mathrm{so}}=0$, the DOS for spin ''up'' (dashed line) and the one for spin ''down'' (solid line) are shifted by $2\mu_B H$ and the Zeeman splitting is clearly visible. The increase of the value of b_{so} leads to a spin-mixing effect on the density of states and for very short spin-orbit scattering times, i.e., $\tau_{\mathrm{so}}\Delta\ll 1$, the Zeeman splitting is no longer observable. Because of its effects on the quasiparticle DOS, b_{so} can be experimentally determined by measurements of the conductance of tunneling junctions,[15] and the same holds true for the depairing parameter ζ.[18]

III. KINETIC EQUATIONS

A superconductor can be driven out of equilibrium by different sources.[10] In a nonequilibrium situation, the quasiparticle and phonon distributions $f_\sigma(\mathbf{k},E_\mathbf{k})$ and $n(\mathbf{q},\omega_q)$ will differ from their form at equilibrium in a way which critically depends on the particular mechanism responsible for the nonequilibrium state. Here, we are interested in the energy resolved nonequilibrium distributions $f_\sigma(E)$ and $n(\omega)$ resulting from the effect of quasiparticle and phonon injection into a superconducting film under the influence of an applied magnetic field H. A Green's functions formalism can be suitably defined in order to deal with nonequilibrium systems.[25] However, here we follow a hybrid procedure by

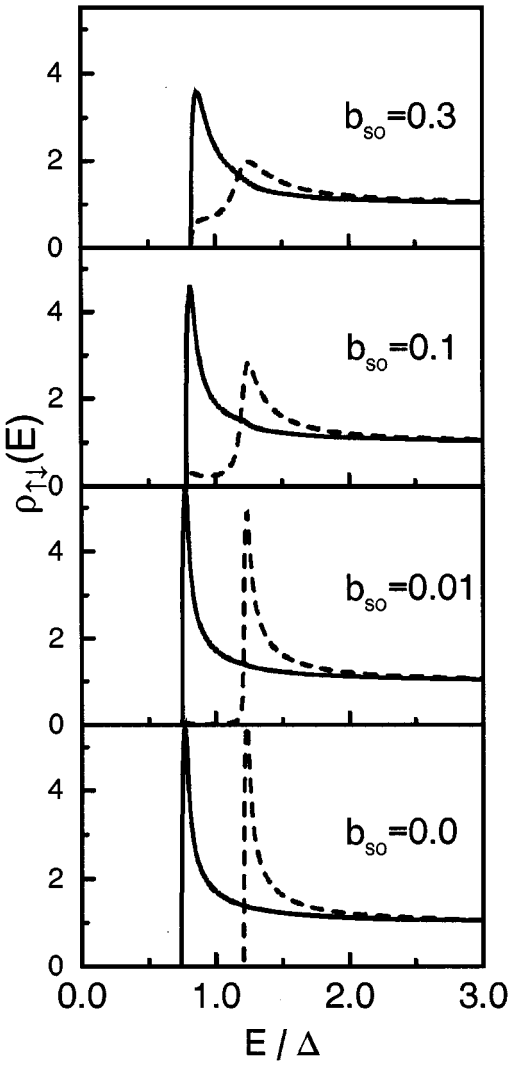

FIG. 1. Quasiparticle density of states for an applied magnetic field of 2 T and different values of the spin-orbit scattering parameter b_{so}. $\rho_{\uparrow}$ and $\rho_{\downarrow}$ are shown by dashed and solid lines, respectively. A small value of the pair-breaking parameter, i.e., $\zeta=0.002$, was introduced in order to smear the singularities for $b_{so}=0$.

making use of Boltzmann-like kinetic equations[10,11] where the self-energy effects arising from the spin-orbit coupling and the influence of the magnetic field on the electron orbits are incorporated in the quasiparticle DOS and in the coherence factors. Since we will focus our analysis on aluminum, i.e., a weak-coupling superconductor, the self-energy effects due to the electron-phonon interaction can be safely neglected. The resulting kinetic equations for the quasiparticle and phonon distributions $f_\sigma(E)$ and $n(\omega)$ are

$$\frac{df_\sigma(E)}{dt}=I_\sigma^{\mathrm{qp,curr}}(E)+I_\sigma^{\mathrm{qp}}(E)+I_{\sigma,\sigma}^{\mathrm{imp}}(E)-\frac{\delta f_\sigma(E)}{\tau_c}, \quad (9)$$

$$\frac{dn(\omega)}{dt}=I^{\mathrm{ph,curr}}(\omega)+\sum_\sigma I_\sigma^{\mathrm{ph}}(\omega)-\frac{\delta n(\omega)}{\tau_{\mathrm{esc}}}. \quad (10)$$

Here, $I_\sigma^{\mathrm{qp,curr}}(E)$ and $I^{\mathrm{ph,curr}}(\omega)$ represent the injection rates for quasiparticles and phonons, respectively. $I_\sigma^{\mathrm{qp}}(E)$ and $I_\sigma^{\mathrm{ph}}(\omega)$ are the collision integrals due to electron-phonon scattering processes and $I_{\sigma,\sigma}^{\mathrm{imp}}(E)$ is the rate of the quasiparticle spin-flip induced by the spin-orbit scattering potential (6). τ_{esc} is the escape time of the phonons due to the thermal coupling between the superconducting film and the thermal reservoir and τ_c is a phenomenological quasiparticle lifetime which will be specified later. The deviation from the equilibrium of quasiparticles and phonons distributions are given by $\delta f_\sigma(E)=f_\sigma(E)-f_0(E,T)$ and $\delta n(\omega)=n(\omega)-n_0(\omega,T)$, respectively, where $f_0(E,T)$ and $n_0(\omega,T)$ are the corresponding equilibrium distributions at temperature T.

The system under consideration consists of phonons and quasiparticles which interact with the magnetic field mainly via the electron magnetic moment. Therefore the set of kinetic equations is composed of three coupled equations: one for the phonons, Eq. (10), and two for the quasiparticles with different spin orientations $f_\uparrow(E)$ and $f_\downarrow(E)$.

In principle, the kinetic equations should be accompanied by the following generalized gap equation:[10,11]

$$\frac{1}{\lambda}=\frac{1}{2}\sum_\sigma \int_0^{\omega_D}\frac{dE}{\Delta}\eta_\sigma(E)[1-2f_\sigma(E)], \quad (11)$$

where λ is the dimensionless electron-phonon coupling constant and ω_D is the Debye energy. In Eq. (11) the effects arising from the depairing and the spin-orbit scattering parameters are included in the function $\eta_\sigma(E)$, which is given by

$$\eta_{\uparrow\downarrow}(E)=\mathrm{sgn}(E)\,\mathrm{Re}\left[\frac{1}{(u_\pm^2-1)^{1/2}}\right]. \quad (12)$$

The $u_\pm$ functions have to be evaluated from Eq. (8).

When the superconductor is at equilibrium $f_\sigma(E)=f_0(E,T)$, and Eq. (11) reduces to the ordinary gap equation. On the other hand, when the quasiparticle distribution deviates from its equilibrium form, Eq. (11) gives the modified gap value. If we assume that the deviation $\delta f_\sigma(E)$ of the quasiparticle distribution is small compared to $f_0(E,T)$, then we can evaluate the change $\delta\Delta$ of the order parameter by linearizing Eq. (11) with respect to $\delta\Delta$ and $\delta f_\sigma(E)$. At zero temperature we obtain:[10,11]

$$\frac{\delta\Delta}{\Delta}=-\sum_\sigma \int_0^{\omega_D}\frac{dE}{\Delta}\eta_\sigma(E)\,\delta f_\sigma(E). \quad (13)$$

For the parameters used in our calculations, we find that the maximal value of $|\delta\Delta/\Delta|$ is of the order of 10^{-2}. Therefore we can consistently solve Eqs. (9), (10) by neglecting the change $\delta\Delta$ of the order parameter.

A. Driving mechanisms

In the case of a superconducting tunneling junction, the quasiparticles can be injected into one side of the junction by imposing a voltage difference V between the films. If the injecting film is assumed to be in equilibrium, the quasiparticle injection rate is then given by

$$I_\sigma^{\mathrm{qp,curr}}(E)=A\rho_\sigma(E-eV)[f_0(E-eV,T)-f_\sigma(E)], \quad (14)$$

where we have assumed that the order parameter Δ is the same in the two superconducting films. The prefactor A in the above equation is given by

$$A=\frac{4\pi}{\hbar}|T|^2\Omega N(0)=\frac{1}{e^2\Omega N(0)R_T}. \tag{15}$$

In this equation, T is the tunneling matrix element, Ω is the volume of the film, e is the electronic charge, and R_T is the resistance of the junction. The latter can assume values ranging from about 0.01 to about tens of ohm.

The phonon injection rate $I^{\mathrm{ph,curr}}(\omega)$ becomes important when a STJ is driven out of equilibrium by phonon rather than quasiparticle injection. This is the case when, for example, a heater is attached to a superconducting film or when phonons generated by another STJ are injected into the film. In Sec. IV we will study the latter situation in detail.

B. Electron-phonon collision integrals

The inelastic scattering processes taking place between quasiparticles and phonons are given by the collision integrals $I_\sigma^{\mathrm{qp}}(E)$ and $I_\sigma^{\mathrm{ph}}(\omega)$. For a BCS superconductor, they can be easily obtained by applying Fermi's golden rule.[10,11] As pointed out before, we include the self-energy effects due to τ_{so} and ζ in the DOS and the coherence factors. In this way we obtain

$$\begin{aligned}I_\sigma^{\mathrm{qp}}(E)=&-\frac{2\pi}{\hbar}\int_0^\infty d\omega\alpha^2F(\omega)\rho_\sigma(E+\omega)\mathcal{N}_{\sigma,\sigma}(E,E+\omega)\{f_\sigma(E)[1-f_\sigma(E+\omega)]n(\omega)-f_\sigma(E+\omega)[1-f_\sigma(E)]\\&\times[1+n(\omega)]\}-\frac{2\pi}{\hbar}\int_0^\infty d\omega\alpha^2F(\omega)\rho_\sigma(E-\omega)\mathcal{N}_{\sigma,\sigma}(E,E-\omega)\{f_\sigma(E)[1-f_\sigma(E-\omega)][1+n(\omega)]-f_\sigma(E-\omega)[1\\&-f_\sigma(E)]n(\omega)\}-\frac{2\pi}{\hbar}\int_0^\infty d\omega\alpha^2F(\omega)\rho_{\bar\sigma}(\omega-E)\mathcal{M}_{\sigma,\bar\sigma}(E,\omega-E)\{f_\sigma(E)f_{\bar\sigma}(\omega-E)\\&\times[1+n(\omega)]-[1-f_\sigma(E)][1-f_{\bar\sigma}(\omega-E)]n(\omega)\},\end{aligned} \tag{16}$$

$$\begin{aligned}I_\sigma^{\mathrm{ph}}(\omega)=&-\frac{4\pi}{\hbar}\frac{N(0)}{N}\frac{\alpha^2F(\omega)}{F(\omega)}\int dE\int dE'\rho_\sigma(E)\rho_\sigma(E')\mathcal{N}_{\sigma,\sigma}(E,E')\{f_\sigma(E')[1-f_\sigma(E)]n(\omega)-f_\sigma(E)[1-f_\sigma(E')]\\&\times[1+n(\omega)]\}\delta(E'-E+\omega)-\frac{2\pi}{\hbar}\frac{N(0)}{N}\frac{\alpha^2F(\omega)}{F(\omega)}\int dE\int dE'\rho_\sigma(E)\rho_{\bar\sigma}(E')\mathcal{M}_{\sigma,\bar\sigma}(E,E')\\&\times\{[1-f_\sigma(E)][1-f_{\bar\sigma}(E')]n(\omega)-f_\sigma(E)f_{\bar\sigma}(E')[1+n(\omega)]\}\delta(E+E'-\omega).\end{aligned} \tag{17}$$

In the above equations, $\alpha^2F(\omega)$ is the Eliashberg function for the electron-phonon interaction, $F(\omega)$ is the phonon density of states, and N is the ion density. In our analysis, we consider a weak-coupling superconductor for which the gap function Δ is much smaller than the Debye energy ω_D. For aluminum films of 30 Å, $\omega_D=38$ meV and $\Delta\simeq0.5$ meV,[19] and this condition is well satisfied. Moreover, in the nonequilibrium case, the other important energy scale is the applied voltage eV which we consider to be always less than 6Δ. Therefore, we can safely approximate the Eliashberg function and the phonon DOS by their low-energy limits[26]

$$\alpha^2F(\omega)=b\omega^2, \tag{18}$$

$$F(\omega)=a\omega^2. \tag{19}$$

For aluminum $b\simeq0.317\times10^{-3}$ meV^{-2} and $a\simeq0.18\times10^{-3}$ meV^{-3}.[12,26]

In the collision integrals (16) and (17), $\rho_\sigma(E)$ is the quasiparticle DOS defined by Eqs. (2), (8) and the functions $\mathcal{N}_{\sigma,\sigma}(E,E')$ and $\mathcal{M}_{\sigma,\bar\sigma}(E,E')$ are the coherence factors for quasiparticle scattering and quasiparticle recombination and/or creation, respectively. The quasiparticle-phonon scattering is a single-electron and spin-conserving process while a recombination (creation) process involves two quasiparticles (holes). Because of the singlet nature of the pairing state $(\mathbf{k}\uparrow,-\mathbf{k}\downarrow)$ the quasiparticles must have opposite spin orientations in order to recombine in the Cooper pair, and therefore the associated coherence factor $\mathcal{M}_{\sigma,\bar\sigma}(E,E')$ depends on two opposite spin eigenvalues.

For a BCS superconductor for which the presence of an external magnetic field H influences only the spin degrees of freedom through the Zeeman splitting ($b_{\mathrm{so}}=0$, $\zeta=0$), the coherence factors are given by

$$\mathcal{N}_{\sigma,\sigma}(E,E')=\frac{1}{2}\left[1-\frac{\Delta^2}{(E-\sigma\mu H)(E'-\sigma\mu H)}\right], \tag{20}$$

$$\mathcal{M}_{\sigma,\bar\sigma}(E,E')=\frac{1}{2}\left[1+\frac{\Delta^2}{(E-\sigma\mu H)(E'+\sigma\mu H)}\right]. \tag{21}$$

However, for finite values of the spin-orbit scattering and depairing parameters ($b_{\mathrm{so}}\neq0$, $\zeta\neq0$), a more general form of the coherence factors is given by the following expressions:

$$\mathcal{N}_{\sigma,\sigma}(E,E')=\frac{1}{2}\left[1-\frac{\eta_\sigma(E)\,\eta_\sigma(E')}{\rho_\sigma(E)\rho_\sigma(E')}\right], \tag{22}$$

$$\mathcal{M}_{\sigma,\bar{\sigma}}(E,E')=\frac{1}{2}\left[1+\frac{\eta_\sigma(E)\,\eta_{\bar{\sigma}}(E')}{\rho_\sigma(E)\rho_{\bar{\sigma}}(E')}\right], \tag{23}$$

where $\rho_\sigma(E)$ and $\eta_\sigma(E)$ are given by Eq. (2) and Eq. (12), respectively. For $\zeta\to 0$ and $b_{\rm so}\to 0$ Eq. (22) reduces to the BCS limit Eq. (20).

The order of magnitude of the collision integrals $I_\sigma^{\rm qp}(E)$ and $I_\sigma^{\rm ph}(\omega)$ can be obtained by rescaling the quasiparticle and phonon energies with the order parameter Δ. In this way we obtain $I_\sigma^{\rm qp}(E)=(\tau_0^{\rm qp})^{-1}\overline{I_\sigma^{\rm qp}}(\overline{E})$ and $I_\sigma^{\rm ph}(\omega)=(\tau_0^{\rm ph})^{-1}\overline{I_\sigma^{\rm ph}}(\overline{\omega})$, where $\overline{\omega}=\omega/\Delta$, $\overline{E}=E/\Delta$ and $\overline{I_\sigma^{\rm qp}}(\overline{E})$ and $\overline{I_\sigma^{\rm ph}}(\overline{\omega})$ are dimensionless electron-phonon collision integrals. The characteristic rates $(\tau_0^{\rm qp})^{-1}$ and $(\tau_0^{\rm ph})^{-1}$ are given below

$$(\tau_0^{\rm qp})^{-1}=\frac{2\pi}{\hbar}b\Delta^3, \tag{24}$$

$$(\tau_0^{\rm ph})^{-1}=\frac{2\pi}{\hbar}\frac{N(0)}{N}\frac{b}{a}\Delta, \tag{25}$$

where we used Eqs. (18)-(19) for the Eliashberg function and the phonon density of states. By making use of the values of a and b given above, and of $N(0)/N\simeq 2.03\times 10^{-4}$ meV^{-1},[12,26] we find for $\Delta\simeq 0.5$ meV, $(\tau_0^{\rm qp})^{-1}\simeq 3.8\times 10^8$ sec^{-1} and $(\tau_0^{\rm ph})^{-1}\simeq 1.7\times 10^9$ sec^{-1}.

In addition to the electron-phonon interaction, the quasiparticles undergo inelastic scattering and recombination (creation) processes via the electron-electron interaction. The associated collision integral is rather cumbersome[27] and usually, in calculating the nonequilibrium distribution functions $f_\sigma(E)$ and $n(\omega)$, its contribution is ignored.[9–12] Moreover, in order to establish a voltage difference and to detect a tunneling current, STJ's are connected to a circuit. Therefore the quasiparticles have a finite probability to escape from the film before they interact with the phonons or with the spin-orbit scattering centers. We decided to simulate these effects in the simplest way by introducing a phenomenological quasiparticle lifetime τ_c in Eq. (9). We would like to stress that the Coulomb contribution to τ_c is not to be confused with the electron-electron scattering time at equilibrium but rather has to be interpreted as a nonequilibrium lifetime. In fact, at equilibrium and at zero temperature, all electrons near the Fermi surface are condensed into Cooper pairs. If we add a quasiparticle, this will have an infinite equilibrium electron-electron relaxation time because there are no other quasiparticles to interact with. In this case, only recombination transitions contribute to the electron-electron scattering time. Instead, under a nonequilibrium condition such as injection of quasiparticles, the quasiparticle population is increased and there will be a finite contribution of the relaxation processes to the electron-electron lifetime.[28] Because of the phenomenological nature of τ_c, its value is fixed by the experimental data in the way described in the next section.

C. Spin-orbit collision rate

As we have seen in Sec. II, the presence of the spin-orbit scattering potential (6) can have strong effects on the quasiparticle spectrum leading to spin-mixing features in the quasiparticle DOS. On the other hand, a finite spin-orbit scattering time τ_{so} is also responsible for real processes in which a quasiparticle with initial spin state σ is scattered into a final state with reversed spin $\bar{\sigma}=-\sigma$. This scattering is elastic and the final and initial quasiparticle energies are the same. We have included this process in the kinetic equation (9) by introducing the following spin-orbit collision term:[29]

$$I_{\sigma,\bar{\sigma}}^{\rm imp}(E)=-\tau_{\rm so}^{-1}\rho_{\bar{\sigma}}(E)\mathcal{N}_{\sigma,\bar{\sigma}}(E,E)[f_\sigma(E)-f_{\bar{\sigma}}(E)], \tag{26}$$

where τ_{so}^{-1} is the spin-orbit scattering rate given by Eq. (7). When $H\neq 0$ and $\tau_{\rm so}^{-1}\to 0$, the quasiparticle kinetic equations for spin ''up'' and spin ''down'' become decoupled. In this case the nonequilibrium distributions $f_\uparrow(E)$ and $f_\downarrow(E)$ are independent and the superconductor remains spin polarized. However, for finite values of $\tau_{\rm so}^{-1}$, the spin-orbit collision integral (26) leads to a relaxation of the spin-imbalance. We will see in the following that the combined action of the elastic spin-orbit scattering and the electron-phonon interaction is responsible for the interesting features observed in the experiments.[19–21]

The effectiveness of the spin-orbit collision term in changing the spin state of a quasiparticle with energy E depends on the characteristic time of the inelastic processes due to the electron-phonon interaction. The relative strength of the spin-orbit scattering with respect to the electron-phonon one can therefore be estimated by the following quantity:

$$\frac{\tau_0^{\rm qp}}{\tau_{\rm so}}=\frac{\hbar}{2\pi}\frac{\tau_{\rm so}^{-1}}{b\Delta^3}=\frac{b_{\rm so}}{b}\frac{1}{2\pi\Delta^2}, \tag{27}$$

where we used the expression (24) for $(\tau_0^{\rm qp})^{-1}$. For $\Delta\sim 0.5$ meV the above quantity is $\tau_0^{\rm qp}/\tau_{\rm so}\sim 10^3 b_{\rm so}$. By including the reduction due to the coherence factor appearing in Eq. (26), this value is decreased by one order of magnitude for a magnetic field of 2 Tesla. Therefore, also for very small values of the spin-orbit scattering parameter, i.e., $b_{\rm so}\sim 0.01$, the quantity in Eq. (27) can be of order unity. It is worth noticing that, for the value of $b_{\rm so}$ used in the above estimate, the quasiparticle DOS deviates slightly from the form expected in the absence of spin-orbit scattering. This can be seen by comparing in Fig. 1 the DOS calculated for $b_{\rm so}=0$ with the one obtained for $b_{\rm so}=0.01$.

In the numerical analysis of the kinetic equations (9) and (10) we shall consider different values of the spin-orbit scattering parameter $b_{\rm so}$ in order to study its effect on the nonequilibrium properties of a superconductor. Experimentally this kind of analysis can be achieved by varying the concentration of impurities in the sample. Meservey *et al.*[18] were able to prepare good quality Al tunneling junctions with Mn impurities in a wide range of Mn concentrations. In this way they were able to modify the value of $b_{\rm so}$.

D. Phonon escape time

The last term in Eq. (10) is the phonon escape rate due to the coupling between the superconducting film and the thermal reservoir. $\tau_{\rm esc}$ is a quantity which depends on the specific material and on the geometry of the junction, and is proportional to the thickness of the film. Following Refs. 8,11,12, the rate of the phonon escape from a thin film is given as

$$\tau_{\rm esc}^{-1}=\frac{\alpha_t v_s}{4d}, \tag{28}$$

where v_s is the velocity of sound, d is the thickness of the film, and α_t is the phonon transmission coefficient. We treat $\tau_{\rm esc}$ as a phenomenological quantity, and in this perspective also the anharmonic effects due to the phonon-phonon interaction can be included in it. A useful quantity in evaluating the effectiveness of $\tau_{\rm esc}$ is the ratio $\tau_0^{\rm ph}/\tau_{\rm esc}$ where $\tau_0^{\rm ph}$ is the characteristic lifetime for the electron-phonon interaction in the phonon channel displayed in Eq. (25). When $\tau_0^{\rm ph}/\tau_{\rm esc}$ diverges ($\tau_{\rm esc}\rightarrow 0$) the steady-state solution of Eq. (10) is $n(\omega)=n_0(\omega)$ and therefore the quasiparticles are coupled to a thermal bath in equilibrium. On the other hand, with the increase of $\tau_{\rm esc}$ a nonequilibrium distribution of phonons sets in, meaning that the system is under the effect of an external source injecting quasiparticles or/and phonons.

IV. RESULTS AND DISCUSSION

The steady-state nonequilibrium quasiparticle and phonon distributions are obtained by imposing the stationary conditions $df_\sigma(E)/dt=0$ and $dn(\omega)/dt=0$ on the kinetic equations (9) and (10). The numerical solution is then achieved by transforming the integrals appearing in Eqs. (16)–(17) into summations over discrete energy levels E_i and ω_i. In this way the kinetic integral equations reduce to a nonlinear system of equations where the unknown variables are $\delta f_\sigma(E_i)=f_\sigma(E_i)-f_0(E_i,T)$ and $\delta n(\omega_i)=n(\omega_i)-n_0(\omega_i,T)$. We introduce a vector $\mathbf{X}$ with components X_i given by

$$X_i=\begin{cases}\delta f_\uparrow(E_i) & i=1,\ldots,n,\\ \delta f_\downarrow(E_i) & i=n+1,\ldots,2n,\\ \delta n(\omega_i) & i=2n+1,\ldots,4n,\end{cases}$$

where $n=MM_d$ with $M=3$, $M_d=45$ and in units of 1 meV the discrete energy levels E_i and ω_i are defined as

$$\begin{aligned}&E_i=(i-1)/M_d, && i=1,\ldots,n,\\ &E_i=(i-n-1)/M_d, && i=n+1,\ldots,2n,\\ &\omega_i=(i-2n-1)/M_d, && i=2n+1,\ldots,4n.\end{aligned}$$

The upper energy cutoffs $E_{\rm max}$ and $\omega_{\rm max}$ are therefore 3 and 6 meV, respectively. They correspond to $E_{\rm max}=6\Delta$ and $\omega_{\rm max}=12\Delta$ for $\Delta=0.5$ meV. The kinetic equations are then solved in the X_i variables by using standard library routines for systems of nonlinear equations. The $u_\pm$ functions entering the DOS and the coherence factors have to be evaluated numerically as well.

Several parameters entering the kinetic equations (9) and (10) depend strongly on the specific tunneling junction. These are the order parameter Δ, the prefactor A in the quasiparticle injection term $I_\sigma^{\rm qp,curr}(E)$, the depairing parameter ζ, the spin-orbit scattering time $\tau_{\rm so}$, the phonon escape time $\tau_{\rm esc}$, and finally the phenomenological electron lifetime τ_c. The first four quantities, namely, Δ, A, ζ and $\tau_{\rm so}$, can be obtained by fitting the calculated tunneling current with the experimental current-voltage characteristics. Here, we have chosen to extract the value of some of these quantities from the experimental data reported in Refs. 19,20 but to let $\tau_{\rm so}$ vary in a certain range of interest. Therefore we put $\Delta=0.5$ meV, and $\tau_0 A=1.25\times 10^{-3}$ which corresponds to $R_T=0.4\Omega$ for an Al film with thickness of 30 Åand cross section 1 mm^2. The depairing parameter ζ, Eq. (4), is proportional to the square of the magnetic field. However, experiments[18] reported that even for $H=0$, ζ has a small but finite value. Therefore ζ should be given by the following expression:[18]

$$\zeta=\zeta_0+C(\mu_B H)^2, \tag{29}$$

where the parameters ζ_0 and C do not depend on the magnetic field. Estimates of the values of ζ_0 and C are obtained as explained above and we find $\zeta_0=0.002$ and $C=0.2$ meV^{-2}. Note also, that for the highest magnetic fields used in this work ($H_{\rm max}=5$ T), the depairing effect is rather small ($\zeta_{\rm max}=0.0188$) and the order parameter can be approximated by its zero field value of 0.5 eV. In performing the numerical calculations, we considered also the situation in which $\zeta=\zeta_0=0.002$, whatever the value of H.

The fit of the current-voltage characteristics does not give information on the values of the phonon escape time $\tau_{\rm esc}$ and the phenomenological quasiparticle lifetime τ_c. We fixed the first quantity by imposing $\tau_0^{\rm ph}/\tau_{\rm esc}=1$, which correspond to an Al film of thickness $d=30$ Å and a phonon transmission coefficient $\alpha_t\simeq 0.7\times 10^{-2}$. The value of τ_c was instead determined in the following way. By looking at the data for the second derivative of the detection current in the phonon spectroscopy experiment reported in Refs. 19–21, we noted that at zero magnetic field, the signals labeled A and B have nearly the same intensity. If $\tau_c^{-1}=0$, a numerical calculation would give an A signal (which results from electron-phonon recombination processes in the generator) much bigger than the B peak (which is due to relaxation processes in the generator). Therefore we tuned the value of τ_c^{-1} in order to obtain nearly the same intensity for the A and B signals at zero magnetic field. In this way, we fixed the value of $\tau_0^{\rm qp}/\tau_c$ to be equal to 3.6 and we kept this value also for magnetic fields different from zero since the H dependence of τ_c should be negligible. As reported in Ref. 21, this assumption led to fairly good agreement with the experimental data.

We solved the coupled kinetic equations (9) and (10) for a superconducting film driven out of equilibrium by quasiparticle injection. This situation is encountered when the superconductor-insulator-superconductor (SIS) junction is biased with a voltage. We also studied a system composed of two equal SIS tunneling junctions separated by a crystal. After traveling through the crystal, the phonons generated by the voltage biased junction can influence the second junction. This is basically the mechanism which permits phonon spectroscopy.

A. Symmetric tunneling junction

In this case the nonequilibrium quasiparticle and phonon distributions are induced by the application of a voltage V through the junction which leads to a quasiparticle injection. Therefore, in the kinetic equations (9) and (10), the phonon current $I^{\rm ph,curr}(\omega)$ is absent and the quasiparticle injection rate is given by Eq. (14). We performed the calculation for

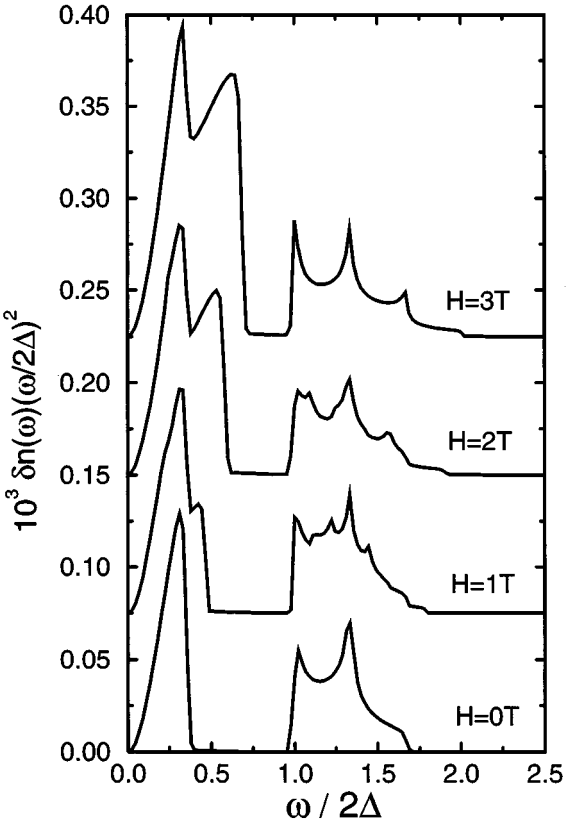

FIG. 2. Phonon emission in the generator STJ for various applied magnetic fields given in Tesla. The applied voltage is $eV/2\Delta = 1.33$ and $\Delta = 0.5$ eV. The spin-orbit scattering parameter is $b_{so} = 0.01$ and the pair-breaking parameter is $\zeta = 0.002$ for all values of the magnetic field. The curves for different values of H have been shifted for clarity.

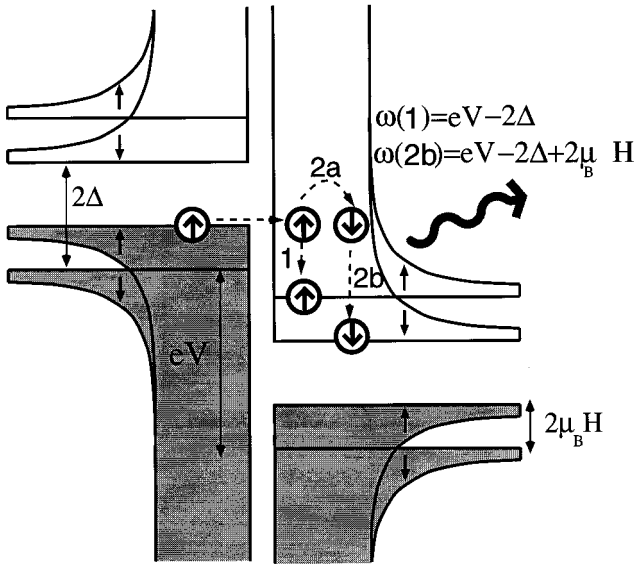

FIG. 3. Quasiparticle relaxation processes for a tunneling junction in an external magnetic field H. The process labeled 1 does not involve spin-flip transitions and gives rise to an emitted phonon with energy of $eV-2\Delta$. The presence of the elastic spin-orbit scattering leads to a spin-flip (process 2a) followed by a relaxation transition by emission of phonons with energy $eV-2\Delta+2\mu_B H$ (process 2b).

different values of the applied magnetic field and of the spin-orbit scattering parameter b_{so}. In this case we set $\zeta=\zeta_0=0.002$, i.e., we neglected the effect of the magnetic field on the electron orbits. Moreover we performed the calculations for a temperature of 0.4 K.

In Fig. 2 we show the calculated deviation of the phonon distribution $\delta n(\omega)=n(\omega)-n_0(\omega,T)$ as a function of the phonon energy. Here the voltage difference is set equal to 1.33 in units of $2\Delta/e$ and the spin-orbit scattering parameter is $b_{so}=0.01$. In zero magnetic field, the injection of quasiparticles cannot produce a spin imbalance and the spin-orbit collision term (26) is zero. The calculated emission phonon spectrum shows a low-energy contribution arising from quasiparticle relaxation processes. This gives rise to emission of phonons up to $\omega\simeq eV-2\Delta$. The spectrum associated with quasiparticle recombination processes has an energy width of approximatively $2eV-4\Delta$ and shows two sharp peaks at $\omega\simeq 2\Delta$ and $\omega\simeq eV$. The former is due to recombination of quasiparticles with energy $E\simeq\Delta$, while the latter corresponds to direct recombination of injected quasiparticles with energy $eV-\Delta$,

As we increase the magnetic field, new structures start to develop in the nonequilibrium phonon spectrum. A second tail, smaller in intensity, is added at energy $eV-2\Delta+2\mu_B H$ while two peaks at $eV\pm 2\mu_B H$ grow at the sides of the main peak at $\omega\simeq eV$. Other tails can be noticed at energies $2eV-2\Delta\pm 2\mu_B H$. Because b_{so} is very small, these features cannot be merely ascribed to the spin-mixing influence on the DOS. Instead, their origin is due to the presence of the spin-orbit collision term (26). In order to clarify this point, we show in Figs. 3 and 4 the physical processes that lead to some of the just mentioned features. In Fig. 3, the Zeeman-split density of states for both films of the junction is displayed in the usual semiconductor representation. If the junction is biased with a voltage V, then quasiparticles can tunnel from one side of the junction to the other. Let us consider the tunneling process of a quasiparticle with spin ''up'' as shown in the figure. After the tunneling, the quasiparticle can relax to the lower permitted energy states by emitting phonons with energies up to $eV-2\Delta$. This transition does not involve spin-flip processes and gives rise to field-independent low-energy contributions in the phonon emission spectrum. However, the presence of the spin-orbit collision integral (26) gives rise to the possibility of a different relaxation process: the tunneled quasiparticle can undergo a spin-flip transition and relax by the emission of phonons. But in this case the maximum phonon energy involved in the process is $eV-2\Delta+2\mu_B H$, therefore, the nonequilibrium phonon spectrum shows a tail at that energy as in Fig. 2. The features associated with the recombination processes have an interpretation similar to the one given above. In Fig. 4, the recombination processes are depicted as quasiparticle transitions from the empty to filled state. Spin-conserving transitions give rise to emission of phonons with energy eV, while the combined action of the spin-orbit elastic scattering and the electron-phonon interaction leads to recombination processes with emission of phonons of energy $eV+2\mu_B H$, Fig. 4(a), and $eV-2\mu_B H$, Fig. 4(b).

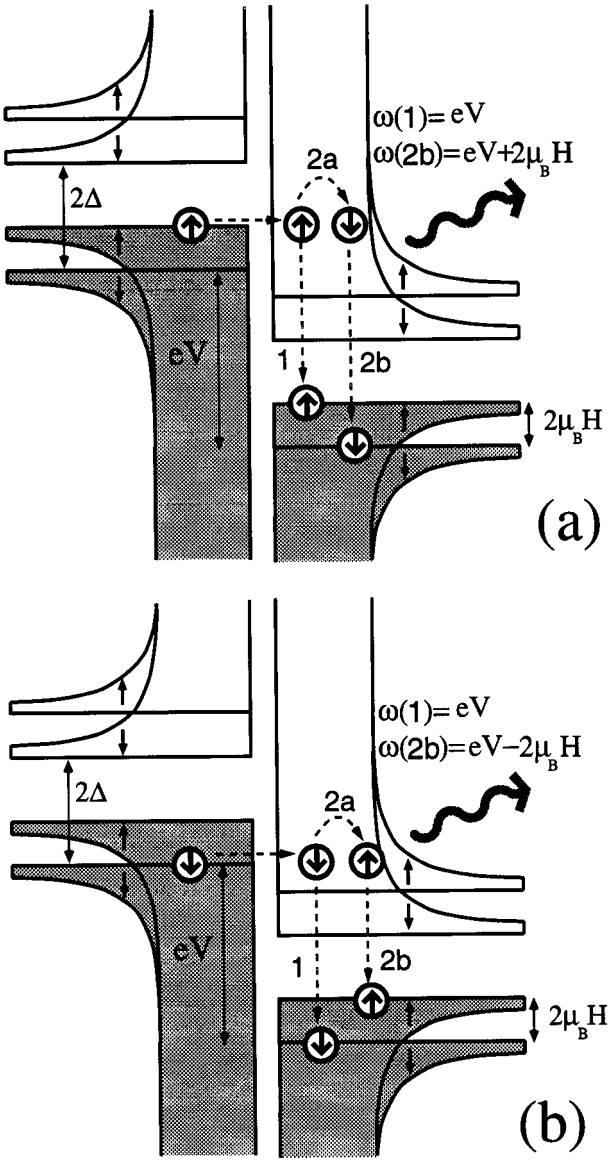

FIG. 4. Recombination processes in the semiconductor representation of the excitations in a tunneling junction. When a quasiparticle undergoes a spin-flip transition it can recombine by emitting phonons with energy $eV+2\mu_B H$ (a) or $eV-2\mu_B H$ (b).

The main effect of a nonzero spin-orbit collision term (26) is therefore the opening of new channels for relaxation and recombination processes. This leads, together with the above mentioned features, to an increase of the total amount of emitted phonons with the magnetic field. We define the integrated emission spectrum of phonons as:

$$S(H)=\int_0^\infty d\omega F(\omega)\delta n(\omega), \tag{30}$$

where H is the magnetic field and $F(\omega)$ is the phonon density of states in the low-energy limit (19). In Fig. 5 we show the numerical results for $S(H)$ normalized to its value at $H=0$ and for $eV/2\Delta=1.33$ and $b_{so}=0.01$. The increase of the magnetic field leads to a clear enhancement of $S(H)$. In our analysis we used a Debye model for the phonon spectrum with no distinction between longitudinal and transverse modes. However, in Al and for small phonon energies, the coupling of the electrons to the transverse phonon modes is stronger than the coupling to the longitudinal ones.[8] Therefore, if we decompose $S(H)$ in its longitudinal and transverse components $S_l(H)$ and $S_t(H)$, respectively, we obtain that $S_t(H)>S_l(H)$. This gives an interpretation of the phonon-pulse measurements reported in Ref. 19, where it was observed that the detection signal for the transverse modes increased more strongly with the magnetic field than the detection signal associated with the longitudinal mode.

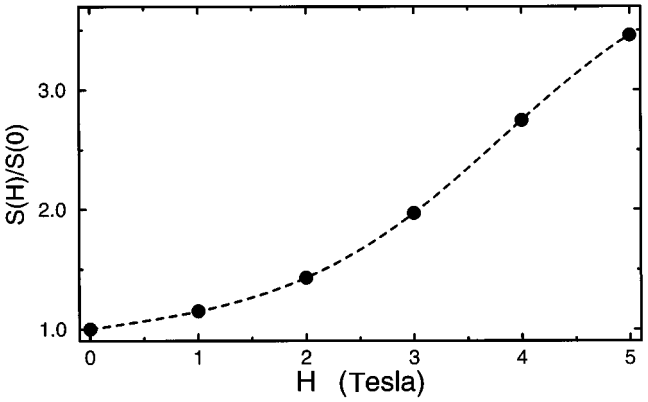

FIG. 5. Integrated emission phonon spectrum normalized at $H=0$. The spin-orbit scattering parameter is $b_{so}=0.01$ and the applied voltage is $eV/2\Delta=1.33$. The dashed line is a guide to the eye.

The nonequilibrium quasiparticle distributions are showed in Fig. 6. Here, $\delta f_\uparrow(E)$ and $\delta f_\downarrow(E)$ are represented by dashed and solid lines, respectively, and the parameters are the same as in Fig. 2. At zero magnetic field the distributions for different spins merge together and the width of the spectrum is approximatively $eV-2\Delta$. The increase of the magnetic field leads to a broadening of the width which is approximatively $eV-2\Delta+2\mu_B H$ for single spin quasiparticle distribution. Also in this case, because of the smallness of b_{so}, this behavior can be understood as resulting from elastic spin-flip transitions due to Eq. (26) rather than from processes involving the spin-mixing states in the Zeeman split quasiparticle DOS. This can be easily seen in the example reported in Fig. 3 where the spin-flip process labeled by 2a increases the width of the spin ''down'' quasiparticle excitations by $2\mu_B H$.

The calculations presented above were performed by using a rather small value of the spin-orbit scattering parameter, namely, $b_{so}=0.01$. By increasing b_{so}, and therefore τ_{so}^{-1}, the scattering rate for spin-flip transitions (26) increases, and the magnetic-field-dependent features described above should become more pronounced. On the other hand, as shown in Fig. 1, the increase of the spin-orbit parameter b_{so} lowers the intensity of the peaks of the quasiparticle DOS and enhances the amount of spin-mixed states for energies below $E\simeq\Delta+\mu_B H$. Moreover, for the same reason, the spin-imbalance of the injected quasiparticles is depressed. As shown in Fig. 7, an increase of b_{so} leads to a smearing of the structures of the emission phonon spectrum associated with the elastic spin-flip transitions. Moreover, the lowering of the DOS peaks also suppresses the structures associated with the transitions without spin-flips, as in the peaks at $\omega\simeq 2\Delta$ and

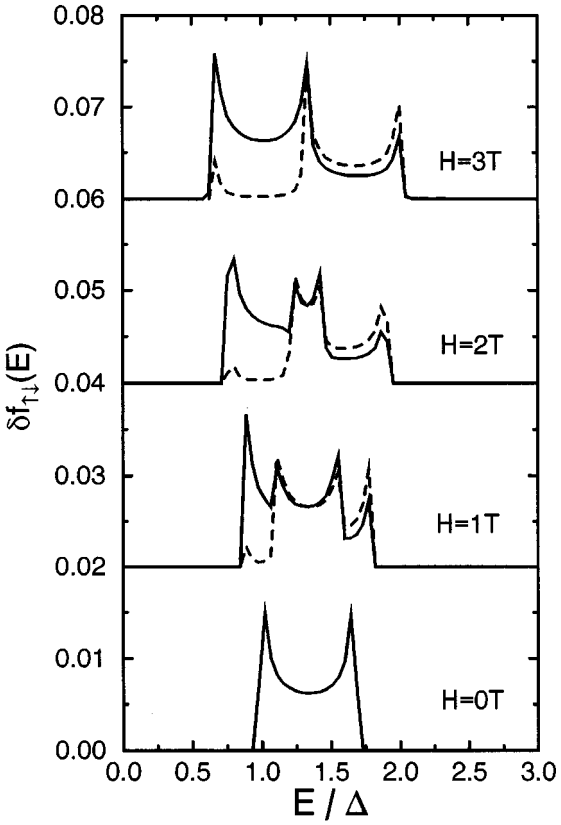

FIG. 6. Nonequilibrium quasiparticle distribution in the generator STJ for $eV/2\Delta = 1.33$ and for different magnetic fields. Here the spin-orbit scattering parameter is $b_{so} = 0.01$ and the spin ''up'' and spin ''down'' quasiparticle distribution functions are given by dashed and solid lines, respectively. The curves for different values of H have been shifted for clarity.

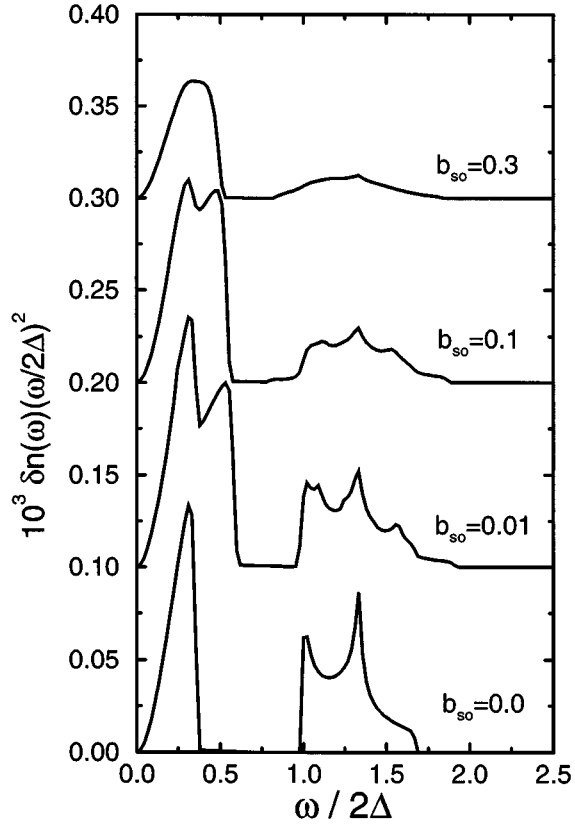

FIG. 7. Phonon emission in the generator STJ for different values of the spin-orbit scattering parameter b_{so}. The curves have been shifted for clarity. The applied magnetic fields is $H = 2$ T and $eV/2\Delta = 1.33$. For $b_{so} = 0.3$, the structures associated with spin-flip transitions are considerably smeared because of the presence of spin-mixed states and the reduction of the peaks in the quasiparticle DOS. The latter effect leads also to a reduction in intensity of the field independent structures such as the peak at $\omega \simeq eV$.

$\omega \simeq eV$. Both the increase of the spin-flip scattering rate and the DOS effects lead to a weakening of the differences between $\delta f_{\uparrow}(E)$ and $\delta f_{\downarrow}(E)$ as shown in Fig. 8. In the limit $\tau_{so} \to 0$, a quasiparticle has the same probability for each of the two spin states, and therefore the quasiparticle and phonon distributions will be indistinguishable from the ones in zero magnetic field.

B. Phonon spectroscopy

In Refs. 19,20 the results of a phonon spectroscopy experiment are reported under the influence of an external magnetic field. A theoretical interpretation of the experimental results has already been given elsewhere.[21] Here we analyze in more detail the physical mechanisms which account for the experimental findings.

As we have seen in the previous analysis, in superconducting tunneling junctions a nonequilibrium population of phonons can set in under quasiparticle injection. If the superconducting film is thermally coupled to the environment (through the phonon escape time τ_{esc}) these nonequilibrium phonons can eventually be emitted from the film. In this way the STJ behaves as a phonon emitter or phonon generator. On the other hand, a STJ can also be exposed to phonon rather than quasiparticle injection. If we suppose that the temperature is zero, then an injected phonon with an energy larger than 2Δ can be absorbed by breaking a Cooper pair. This process leads to an enhancement of the quasiparticle population in that side of the junction which is exposed to the phonon source and, consequently, establishes a potential difference between the two films of the junction. Therefore this phonon absorption process can be detected by measuring the tunneling current induced by the potential difference through the STJ junction.

One of the different techniques used for phonon spectroscopy is based on the principle of phonon emission and absorption in tunneling junctions. Two STJ's are placed on opposite sides of a crystal with a phonon transmission coefficient Γ_t. One STJ (generator) is biased with a voltage V_G and the emitted phonons are absorbed in a second STJ (detector) after crossing the crystal. Measuring the current I_D in the detector junction gives information on the resonant phonon frequencies in the crystal.

A theoretical description of this double junction system is carried out by making use of the kinetic equations for both generator and detector STJ's coupled together by the phonon transmission coefficient Γ_t which simulates the presence of the crystal. Therefore, for the generator tunnel junction, we use the kinetic equations (9) and (10) where $I_{\sigma}^{qp,curr}(E)$ is given by Eq. (14) and $I^{ph,curr}(\omega)$ is zero. In the steady-state

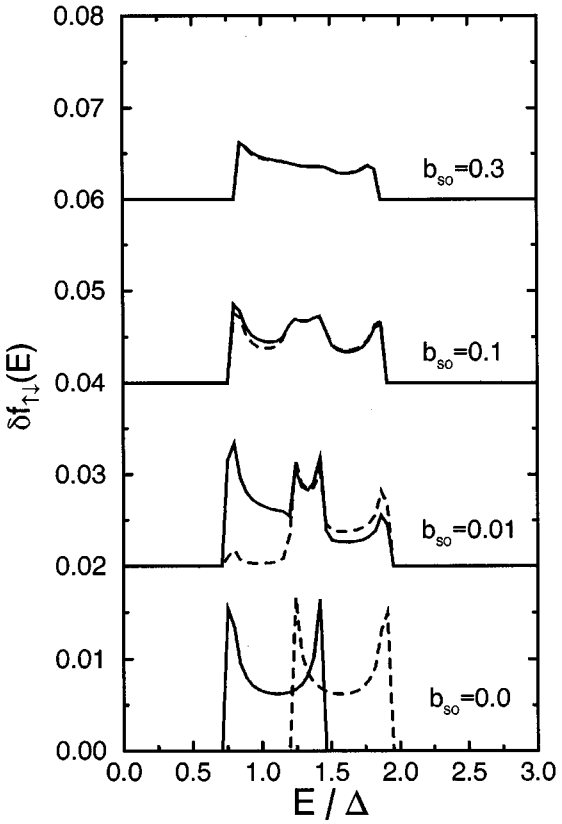

FIG. 8. Nonequilibrium distributions of quasiparticles with spin ''down'' (solid line) and spin ''up'' (dashed line) for different values of the spin-orbit scattering parameter b_{so}. The applied magnetic field is $H=2$ T and $eV/2\Delta=1.33$.

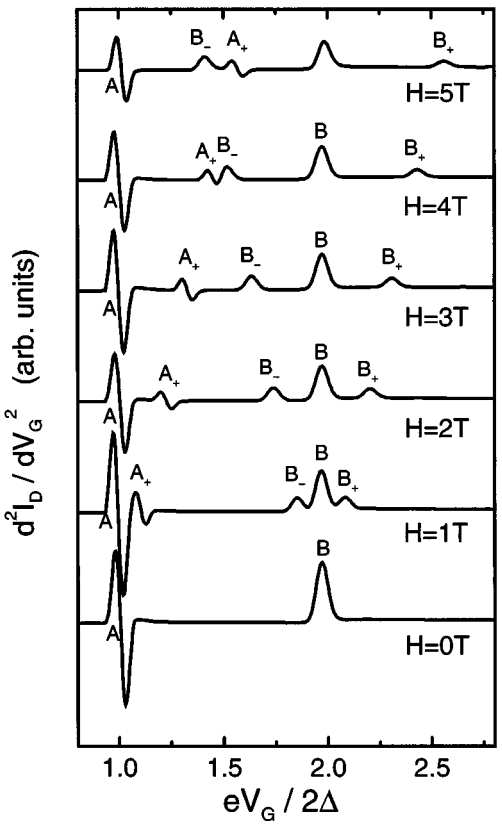

FIG. 9. Second derivative of the detector current I_D with respect to the generator voltage V_G for different applied magnetic fields given in Tesla. The curves for different values of H are shifted vertically for clarity. The spin-orbit scattering parameter is $b_{so}=0.01$ and the pair-breaking parameter ζ is set equal to 0.002. The position of the peaks at $eV_G=2\Delta$ (A) and $eV_G=4\Delta$ (B) is field independent while the structures labeled with A_+ and $B_\pm$ depend strongly on the magnetic field.

regime, the solutions are given by $\delta f_\sigma^G(E)$ and $\delta n^G(\omega)$, which represent the deviation from equilibrium of the quasiparticle and phonon distribution in the generator, respectively.

The kinetic equations for the detector tunneling junction are obtained by replacing in Eqs. (9) and (10) the quasiparticle and phonon injection rates by the expressions

$$I_\sigma^{\mathrm{qp,curr}}(E)=-A\rho_\sigma(E)\,\delta f_\sigma^D(E), \tag{31}$$

$$I^{\mathrm{ph,curr}}(\omega)=\Gamma_t\delta n^G(\omega), \tag{32}$$

where $\delta f_\sigma^D(E)$ is the deviation of the quasiparticle distribution from equilibrium in one side of the detector STJ and $\delta n^G(\omega)$ is the nonequilibrium distribution of phonons emitted by the generator. The first equation represents the tunneling rate of the quasiparticles through the junction. Note that at equilibrium this term is zero (no tunneling current). Equation (32) represents the injection rate of the phonons emitted by the generator. The solution of the second system of kinetic equations is given by $\delta f_\sigma^D(E)$ and $\delta n^D(\omega)$. In this way the tunneling current in the detector can be calculated once $\delta f_\sigma^D(E)$ is known.

Before presenting our numerical results, let us briefly describe the qualitative behavior of the detector current I_D when the generator voltage V_G is varied and the magnetic field is set equal to zero. The description of the I_D-V_G characteristics of a double junction system is simplified if we suppose that the crystal allows for phonon transmission of all the energies of interest and that the order parameter Δ is equal for both the junctions. As we have already seen for $eV_G<2\Delta$, no quasiparticles are injected into the generator STJ and therefore no tunneling current flows in the detector. When $eV_G>2\Delta$, phonons resulting from recombination processes are emitted from the generator. These phonons have energies $\omega>2\Delta$ and can be absorbed in the detector junction. Therefore, a sudden increase from $I_D=0$ to $I_D>0$ is observed in the detector as eV_G crosses 2Δ from below. Under appropriate conditions, for $eV_G>2\Delta$, the detected current increases linearly with V_G. When $eV_G>4\Delta$, also the phonons resulting from relaxation processes have energy sufficient to break Cooper's pairs in the detector, and I_D increases its slope. The sudden enhancement of I_D for $eV_G=2\Delta$ and $eV_G=4\Delta$ can be emphasized by evaluating the second derivative of I_D with respect to the generator voltage V_G.

If spin-flip processes are forbidden, the qualitative behavior described above remains unchanged even when the double junction system is under the influence of an external magnetic field. However, when $H\neq 0$ we have also seen that for a single STJ, the spin-flip processes induced by an elastic

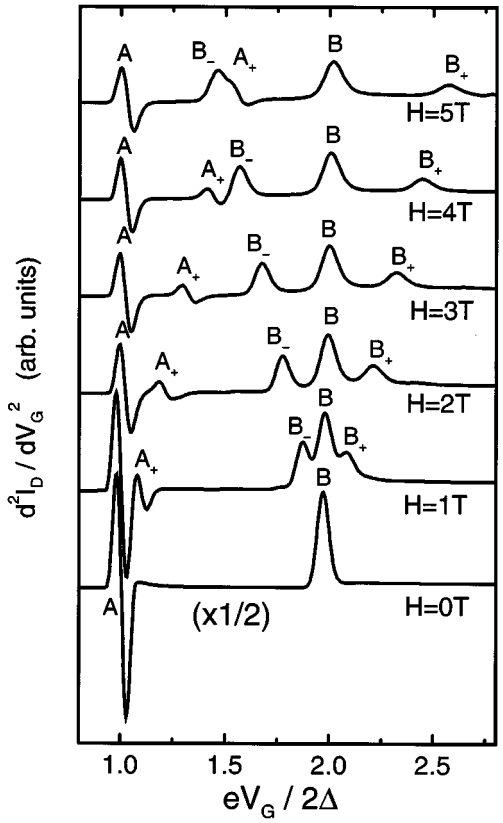

FIG. 10. Second derivative of the detector current I_D with respect to the generator voltage V_G for different applied magnetic fields.The spin-orbit scattering parameter is $b_{so}=0.05$ and the pair-breaking parameter ζ is set equal to 0.002.

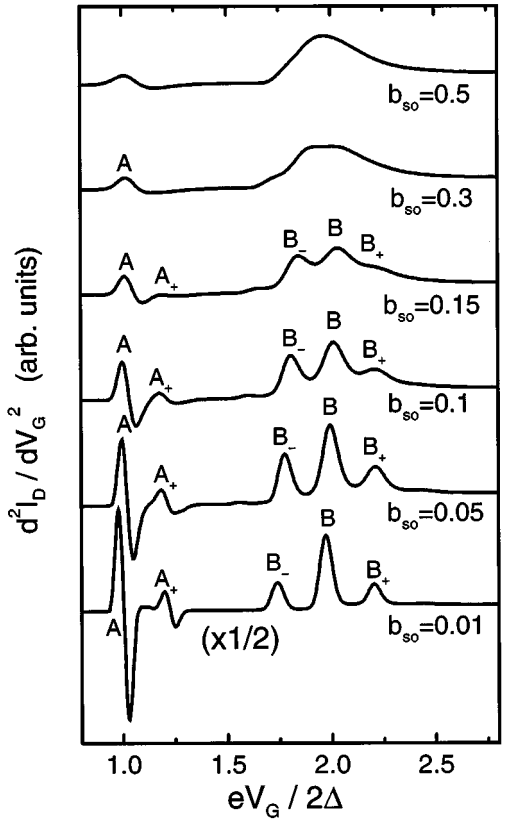

FIG. 11. Effect of the spin-orbit scattering parameter b_{so} on the shape of the peaks. The external magnetic field is $H=2$ T. For $b_{so}=0.5$, the enhancement of the spin-mixed states in the quasiparticle DOS leads to two broad peaks.

spin-orbit scattering strongly modify the nonequilibrium quasiparticle and phonon distributions. Our numerical results are shown in Fig. 9 where d^2I_D/dV_G^2 is plotted for different values of the magnetic field. The spin-orbit scattering parameter is $b_{so}=0.01$ and $\zeta=0.002$. At zero magnetic field the second derivative shows two sharp structures at $eV_G=2\Delta$ (A) and $eV_G=4\Delta$ (B) as expected by the qualitative description given above. The relative intensity of these two structures is tuned by τ_c, and we have fixed this value at 0.5 in order to obtain peaks with approximatively the same intensity as reported in Refs. 19,20.

When the magnetic field is switched on, other structures start to split from the A and B peaks. Their position is given approximatively by $eV_G=2\Delta+2\mu_B H$ for the signal labeled by A_+ and $eV_G=4\Delta\pm2\mu_B H$ for the ones indicated by $B_\pm$.

In Fig. 10 results are reported for $b_{so}=0.05$. The positions of the A_+ and $B_\pm$ peaks are close to the ones shown in Fig. 9. However, the increased value of b_{so} leads to an enhancement of their intensity compared to the A and B signals.

The origin of the A_+ and $B_\pm$ peaks can be completely understood in terms of elastic spin-flip transitions followed by recombination and relaxation processes taking place in the generator junction. For example, the peak at $eV_G=4\Delta-2\mu_B H$ labeled by B_- in Figs. 9,10 is given by the processes labeled by $2a$ and $2b$ in Fig. 3. These transitions generate phonons with energy $\omega(2b)=eV_G-2\Delta-2\mu_B H=2\Delta$ which therefore can be absorbed in the detector STJ and increase the tunneling current I_D. The peaks labeled by B_+ in Figs. 9,10 can be explained in a similar way by considering tunneling of quasiparticles with spin ''down'' in the generator while the A_+ peaks are due to spin-flip transitions followed by recombination processes shown in Fig. 4.

For small values of b_{so}, the field-dependent features in d^2I_D/dV_D^2 can be readily interpreted in terms of elastic spin-flip transitions due to the spin-orbit scattering term given by Eq. (26). For larger values of b_{so}, also the spin-mixed states in the quasiparticle DOS begin to affect the intensity and the shape of the A_+ and $B_\pm$ peaks. In Fig. 11 we report calculations for $H=2\,T$ and for different values of b_{so}. At $b_{so}=0.5$, the structures shown in Figs. 9,10 are no longer visible and only two broad peaks centered around $eV_G\simeq2\Delta$ and $eV_G\simeq4\Delta$ are left. In the limit of $b_{so}\to\infty$, the spin states are completely mixed and d^2I_D/dV_D^2 should be the same as for $H=0\,T$.

Finally, we have also studied the effect of the depairing parameter ζ on d^2I_D/dV_D^2. As we have already pointed out, the finite thickness of the superconducting films in the tunneling junctions leads to a dependence of ζ upon the applied magnetic field as given in Eq. (29). The results are shown in Fig. 12 for $\zeta_0=0.002$ and $C=0.2$ meV^{-2} (solid lines) and compared with the ones obtained for $C=0$ (dotted lines) already displayed in Fig. 10. The reduced sharpness of the quasiparticle DOS caused by ζ, leads to a lowering of the

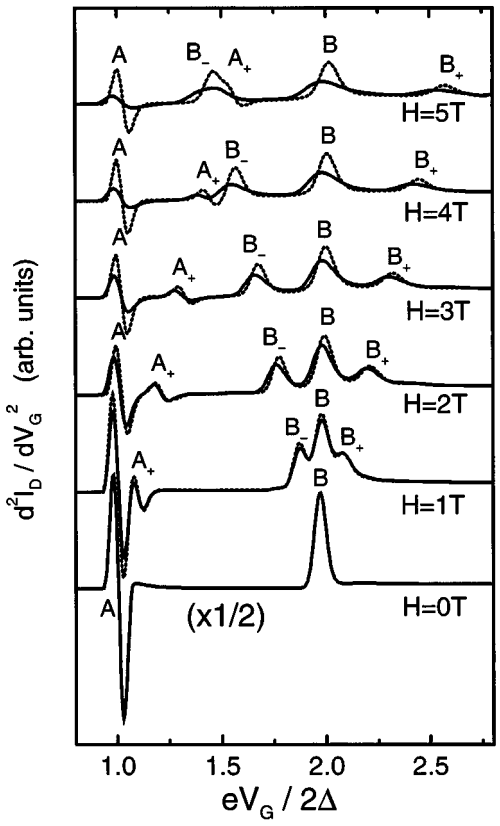

FIG. 12. Effect of the depairing parameter ζ on the second derivative of I_D. Dotted lines are the calculations for $\zeta=0.002$ as in Fig. 10. Solid lines are the results for $\zeta=\zeta_0+C(\mu_B H)^2$ where $\zeta_0=0.002$ and $C=0.2$ meV^{-2}.

intensity of the peaks. Moreover, the position of the peaks is slightly shifted to lower voltages because of the reduced threshold in the density of states. These calculations give good agreements with the experimental data.[19–21]

V. CONCLUSIONS

The results presented in this work show that the inclusion of spin-orbit scattering processes leads to important modifications in the properties of nonequilibrium superconductors in magnetic fields. In particular, the possibility of spin-flip transitions opens new available channels for quasiparticle recombination and relaxation processes. Of course, this would be equally true if, instead of considering spin-orbit scattering, spin-flip transitions with dilute magnetic impurities were taken into account. In this case, the main difference comes from the presence of coherence factors valid for spin-flip scattering processes which break the time-reversal invariance and weight therefore the basic processes depicted in Figs. 3 and 4 in a different way. On the other hand, the situation should change drastically when spin-flip scattering centers are given by Kondo magnetic impurities. In such a case, the present analysis is no longer valid, since the effect of strong electronic correlations has not been taken into account. This is of course an interesting problem worth investigating.

Our numerical analysis also provides an explanation for the experimental findings reported in Ref. 19, and raises interesting questions regarding, for example, the time evolution towards the nonequilibrium state as a function of the magnetic field and the spin-flip scattering rate. In particular, the spin-imbalance relaxation time should present interesting properties when considered in a nonequilibrium situation.

ACKNOWLEDGMENTS

We would like to acknowledge very fruitful and stimulating collaboration with Professor W. Eisenmenger and Dr. J. Lang. We thank Dr. B. Farid, Dr. K. Lassmann, S. Marini, and U. Wenschuh for helpful discussions.

*Present address: I.N.F.M sezione di Roma, Dipartimento di Fisica, Università di Roma ''La Sapienza,'' P.le A. Moro 2, 00185 Roma, Italy.

[1] D. M. Ginsberg, Phys. Rev. Lett. **8**, 204 (1962).
[2] A. Rothwarf and B. N. Taylor, Phys. Rev. Lett. **19**, 27 (1967).
[3] R. C. Dynes, V. Narayanamurti, and J. P. Garno, Phys. Rev. Lett. **41**, 1509 (1978).
[4] W. Eisenmenger and A. H. Dayem, Phys. Rev. Lett. **18**, 125 (1967).
[5] H. Kinder, K. Lassmann, and W. E. Eisenmenger, Phys. Lett. **31A**, 475 (1970).
[6] V. Narayanamurti and R. C. Dynes, Phys. Rev. Lett. **27**, 410 (1971).
[7] A. R. Long and C. J. Adkins, Philos. Mag. **27**, 865 (1973).
[8] W. Eisenmenger, Phys. Acoustic **XII**, 79 (1976).
[9] A. H. Dayem and J. J. Wiegand, Phys. Rev. B **5**, 4390 (1972).
[10] J. J. Chang and D. J. Scalapino, Phys. Rev. B **15**, 2651 (1977).
[11] J. J. Chang and D. J. Scalapino, J. Low Temp. Phys. **31**, 1 (1978); J. J. Chang, in *Nonequilibrium Superconductivity*, edited by D. N. Langenber and A. I. Larkin. (North–Holland, Amsterdam, 1986), p. 453.
[12] A. Zehnder, Phys. Rev. B **52**, 12858 (1995).
[13] J. Cooper, S. Roshko, W. Dietsche, Y. Kershaw, and U. Wenschuh, Phys. Rev. B **50**, 8352 (1994).
[14] R. Meservey, P. M. Tedrow, and P. Fulde, Phys. Rev. Lett. **25**, 1270 (1970).
[15] P. M. Tedrow and R. Meservey, Phys. Rev. Lett. **27**, 919 (1971).
[16] A. A. Abrikosov and L. P. Gorkov, Sov. Phys. JETP **15**, 752 (1962).
[17] P. Fulde, Adv. Phys. **22**, 667 (1973); H. Engler and P. Fulde, Z. Phys. **247**, 1 (1971).
[18] R. Meservey, P. M. Tedrow, and R. C. Bruno, Phys. Rev. B **11**, 4224 (1975).
[19] J. Lang, W. Eisenmenger, and P. Fulde, Phys. Rev. Lett. **77**, 2546 (1996).
[20] J. Lang, Ph.D. thesis, Universität Stuttgart, 1995.
[21] C. Grimaldi and P. Fulde, Phys. Rev. Lett. **77**, 2550 (1996).
[22] K. Maki in *Superconductivity*, edited by R. D. Parks (Dekker, New York, 1969), Vol. 2, p. 1035.
[23] L. P. Gorkov and A. I. Rusinov, Sov. Phys. JETP **19**, 922 (1964).
[24] V. N. Lisin and B. M. Khabibullin, Sov. Phys. Solid State **17**, 1045 (1975).

[25] For a review see, J. Rammer, Rev. Mod. Phys. **58**, 323 (1986), and references therein.

[26] S. B. Kaplan, C. C. Chi, D. N. Langenberg, J. J. Chang, S. Jafarey, and D. J. Scalapino, Phys. Rev. B **14**, 4854 (1976).

[27] G. M. Eliashberg, Sov. Phys. JETP **34**, 668 (1972); A. G. Aronov and B. Z. Spivak, *ibid.* **50**, 328 (1979); V. F. Elesin, *ibid.* **53**, 148 (1981).

[28] Actually, this nonequilibrium lifetime should depend on the nonequilibrium density of quasiparticles.

[29] H. L. Zhao and S. Hershfield, Phys. Rev. B **52**, 3632 (1995).